Electronic Supplementary Material (ESI) for RSC Advances.
This journal is © The Royal Society of Chemistry 2016

A Novel process concept for the three step Boscalid® synthesis

- Supporting Information -

I. Volovych[a], M. Neumann[a], M. Schmidt[a], G. Buchner[a], Ji-Yoon Yang[c], J. Wölk[c], T. Sottmann[b,c], R. Strey[c], R. Schomäcker[a], M. Schwarze[a,d*]

[a]Technische Universität Berlin, Institut für Chemie, Straße des 17 Juni. 124, 10623 Berlin, Germany

[b]Universität Stuttgart, Institut für Physikalische Chemie, Pfaffenwaldring 55, 70569 Stuttgart, Germany

[c]Universität zu Köln, Institut für Physikalische Chemie, Luxemburger Str. 116, 50939 Köln, Germany

[d]Technische Universität Berlin, Institut für Prozess- und Verfahrenstechnik, Straße des 17 Juni. 135, 10623 Berlin, Germany

Corresponding author*: M. Schwarze (ms@chem.tu-berlin.de)

A) Chemical structures of investigated surfactants

The chemical structures of the investigated surfactants are shown in Figure S 1.

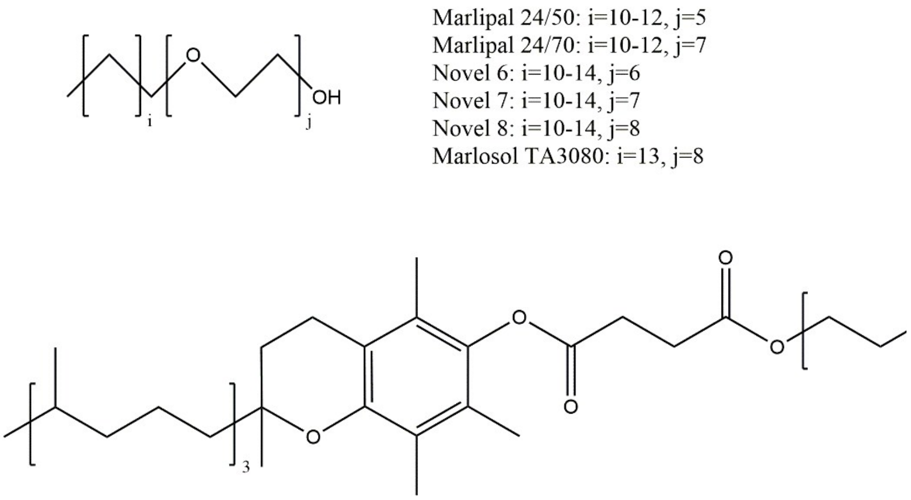

Marlipal 24/50: i=10-12, j=5
Marlipal 24/70: i=10-12, j=7
Novel 6: i=10-14, j=6
Novel 7: i=10-14, j=7
Novel 8: i=10-14, j=8
Marlosol TA3080: i=13, j=8

Figure S 1. Chemical structures of investigated surfactants.

B) Chemical structures of applied ligand and metal precursors

The chemical structures of the Suzuki coupling ligand SPhos and metal precursors for the formulation of the homogeneous catalyst complex or the TiO_2 supported metal catalysts are shown in Figure S 2.

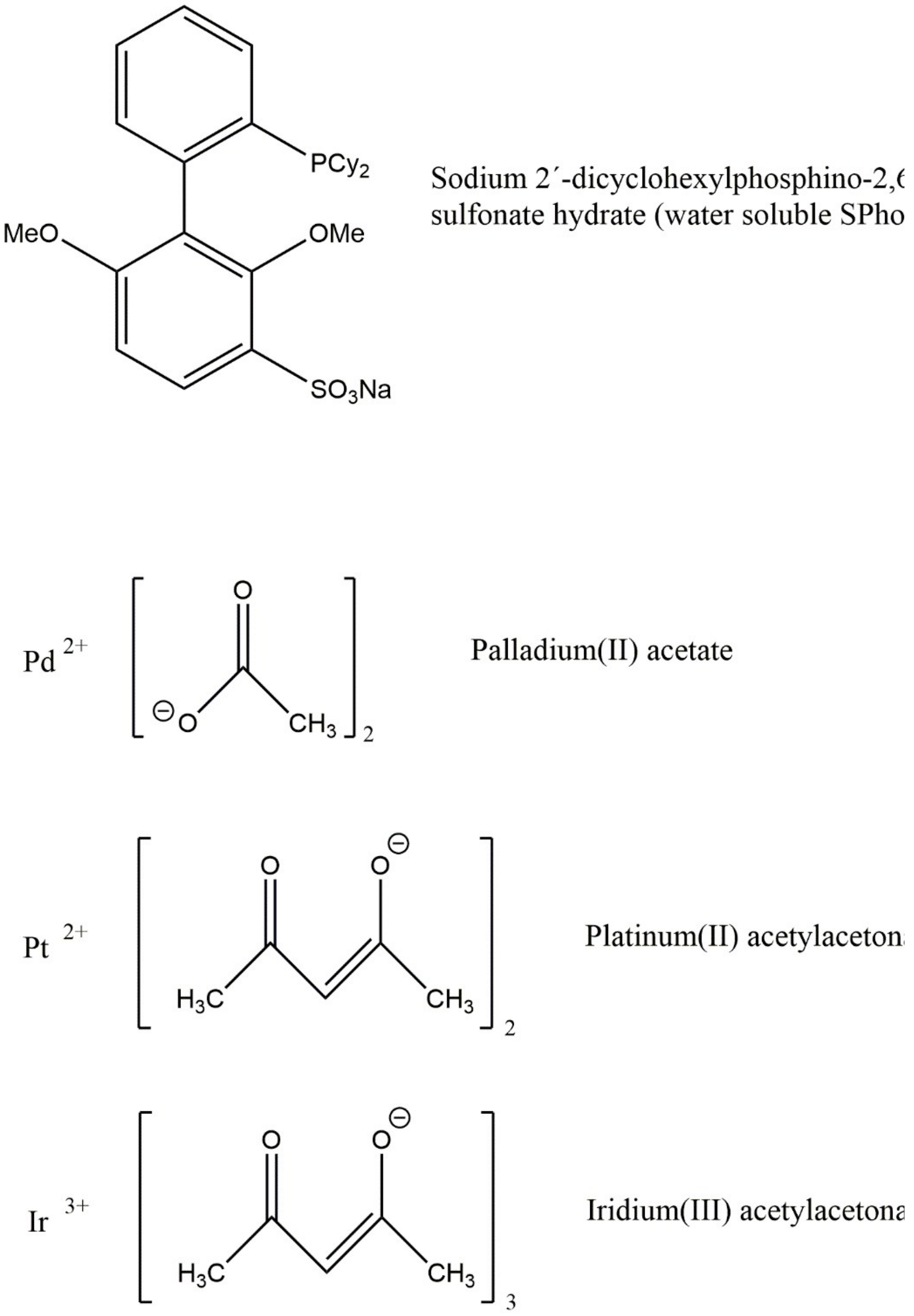

Figure S 2. Chemical structures of SPhos and metal precursors.

C) Microemulsion system

After Suzuki coupling reaction the Pd/SPhos complex stays in the middle phase of the three-phase system. The organic excess phase containing the product is used in the further reactions.

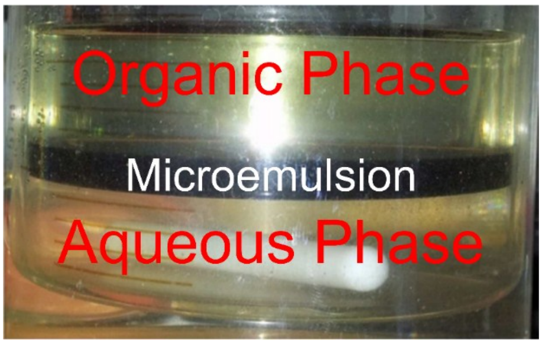

Figure S 3: Three-phase microemulsion system after phase separation with the catalyst complex being located in the middle phase.

D) Characterization of the PtIr@TiO_2 catalyst

For the hydrogenation of the Suzuki coupling product variety of catalysts, either homogeneous or heterogeneous can be utilized. A PtIr@TiO_2 catalyst was applied to obtain a preferably high conversion rate while using only small amounts of noble metal simultaneously. To determine the catalyst properties, such as surface area, crystallite size and Pt content, BET adsorption of N_2 (Micrometrics Gemini, equipped with MI Vac Prep 061) GI-XRD (Bruker D8 advance, equipped with Lynx Eye detector and Cu filament), TEM (FEI Tecnai G2 T20 S-Twin) and ICP-OES (Varian 715 ES) were measured.

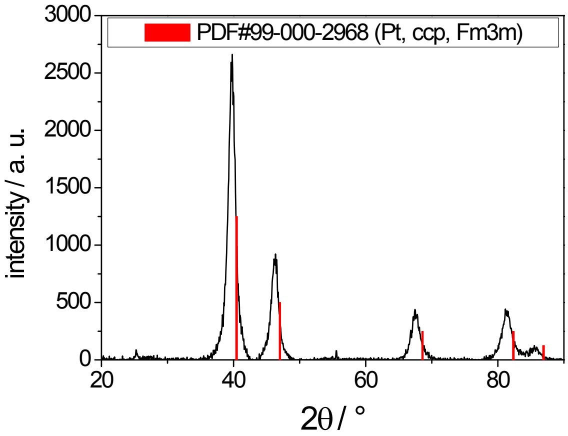

Figure S 4. XRD diffractogram of the PtIr@TiO_2 catalyst (2θ: 20-80°, 0.05°·11s^{-1})

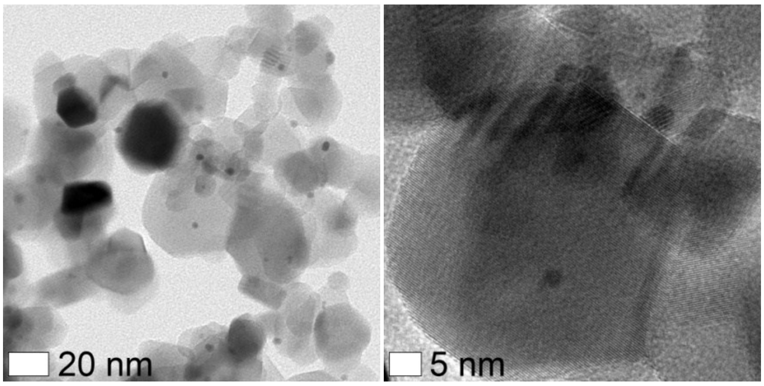

Figure S 5. TEM bright field image of the PtIr@TiO_2 catalyst

The catalyst surface area could be calculated to be 46.4 m²/g. Figure S 3 shows the diffractogram of the PtIr@TiO_2 catalyst, also showing highlighted positions of pure Pt. An average crystallite size of 3.0 nm could be determined. TEM images of the catalyst also indicate a local crystallite size of approximately 2.5 nm (Figure S 4). From ICP-OES investigations the metal content of Pt could be determined to be 0.73 wt%. As a result from the sample preparation using an aqua regia based decomposition method, the effective Ir-content could not be determined. However, a maximum Ir-content of 0.15 wt% is given by the applied Ir-precursor concentration during the synthesis.

E) Setup for hydrogenation reaction

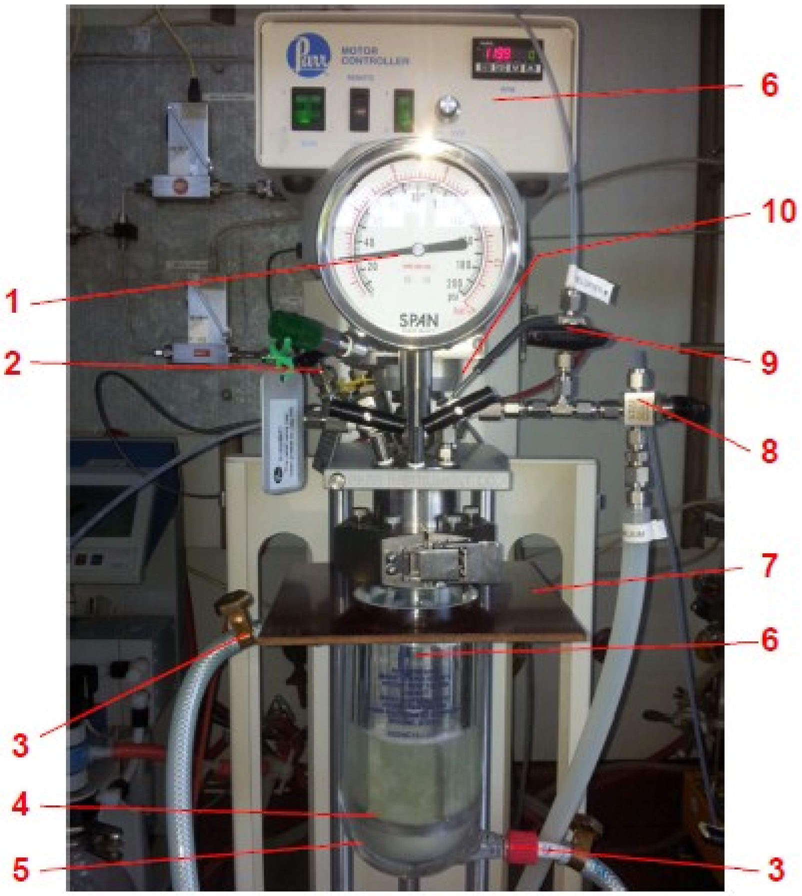

Figure S 6. Setup for hydrogenation experiments. (1) pressure indicator, (2) hydrogen supply, (3) connection to thermostat, (4) baffles, (5) hydrogenation reactor, (6) gas dispersion stirrer, (7) covering plate, (8) nitrogen supply, (9) pressure release, and (10) thermocouple.

F) Preliminary hydrogenation experiments with o-chloro-nitrobenzene

The Suzuki coupling product 4′-chloro-2-nitrobiphenyl is commercially not available. As the hydrogenation of the nitrobiphenyl is the second step within the synthesis of Boscalid®, preliminary experiments were done with a comparable model substrate. Here, o-chloro-nitrobenzene (99% purity, Sigma Aldrich) was selected as reactant to find suitable reaction conditions for the hydrogenation reaction which could be applied later to hydrogenation of 4′-chloro-2-nitrobiphenyl. The reactions were done in a stainless steel autoclave.

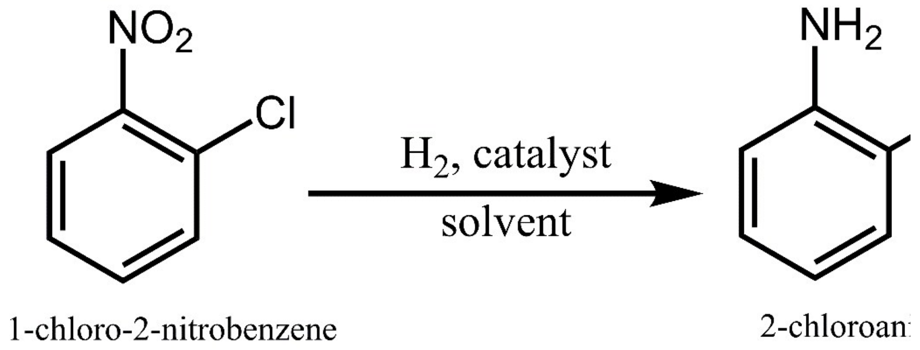

Figure S 7. Scheme for the hydrogenation reaction of 1-chloro-2-nitrobenzene to 2-chloroaniline.

Mainly different supported catalysts based on platinum were synthesized and tested. The results for rate and selectivity are shown in Figure S 7. High selectivity is obtained in all cases (>96 %), but the rate differs. The highest rate was observed for PtIr@TiO_2. This catalyst was selected for the hydrogenation 4′-chloro-2-nitrobiphenyl.

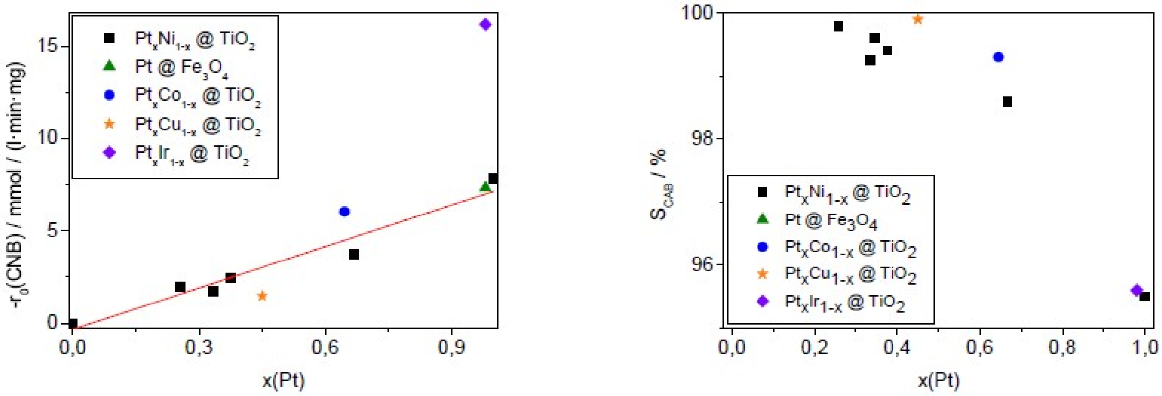

Figure S 8. Rate (a) and selectivity (b) for the hydrogenation of 1-chloro-2-nitrobenzene in ethanol with different supported catalysts based on platinum. Reaction conditions: 15mg catalyst, c_0=0.2 mol/L, T=45 °C, n=2000 rpm, m_{total}=24.77 g, p=10 bar.

G) Influence of solvent

For removal of the produced water from the catalyst surface, a polar solvent is needed. Figure S 7 shows the conversion for the hydrogenation of 4´-chloro-2-nitrobiphenyl in n-heptane, n-heptane/Marlipal 24/70, and water/Marlipal 24/70. Only in the presence of water in the system that dissolve the produced water, high conversions are achievable.

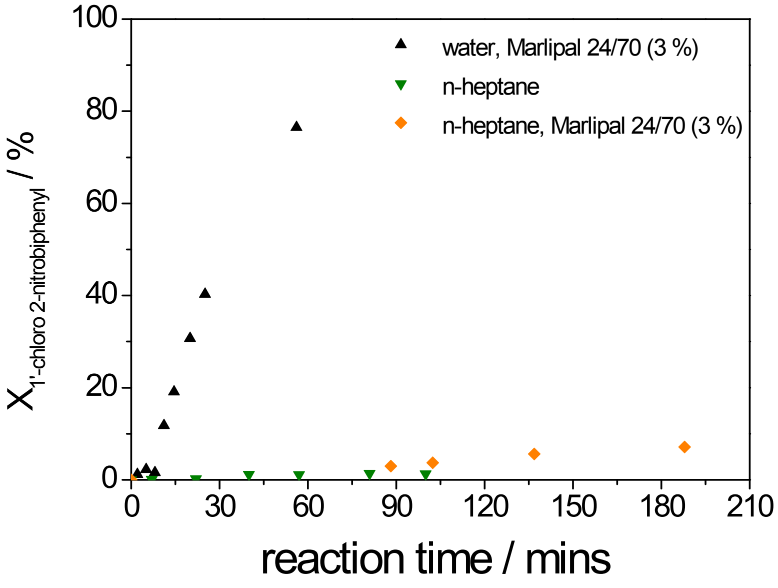

Figure S 9. Hydrogenation of 1’-chloro-2-nitrobenzene with PtIr@TiO_2 (2.31 wt% Pt) in different solvents. Reaction conditions: 15 mg catalyst, c_0=0.1 mol/L, T=60 °C, n=2000 rpm, m_{total}=24.77 g, p=10 bar.

H) Preliminary condensation experiments with 2-aminobiphenyl

To find the best reaction conditions for the condensation reaction to Boscalid, preliminary experiments with 2-aminobiphenly were carried out (Figure S 6).

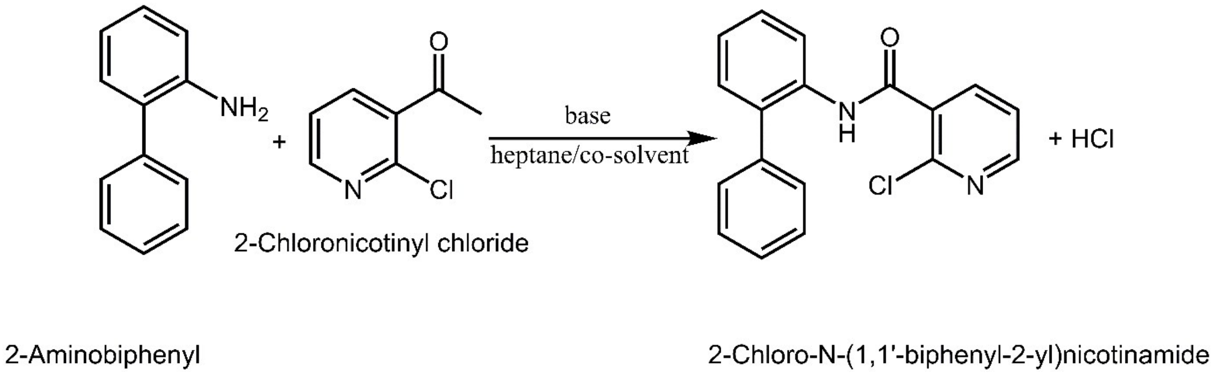

Figure S 10. Scheme for the condensation reaction of 2-aminobiphnyl with 2-chloronicotinyl chloride.

We investigated the influence of the base, the solvent, and the ratio of the reactants on the conversion. The results are shown in Figure S 7 - Figure S 9. As obvious, the base (NEt_3 or pyridine) has no significant influence, but higher CNC concentrations are beneficial.

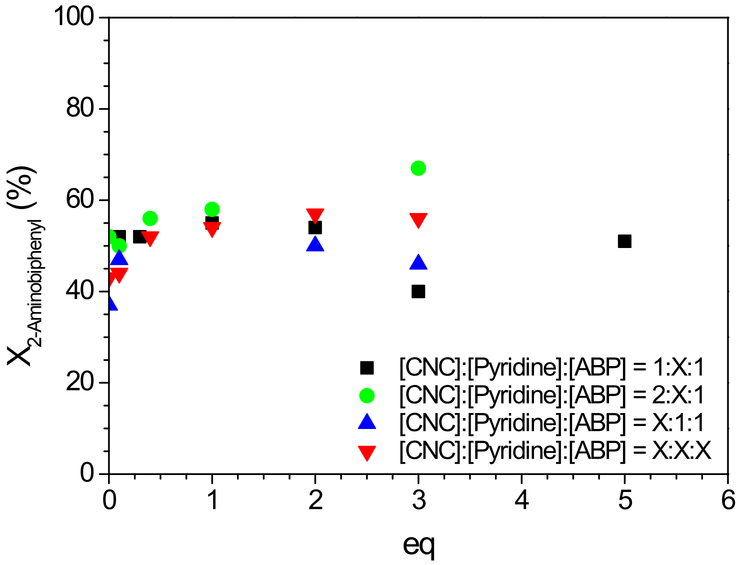

Figure S 11. Influence of reaction composition with pyridine as the base (X=eq).

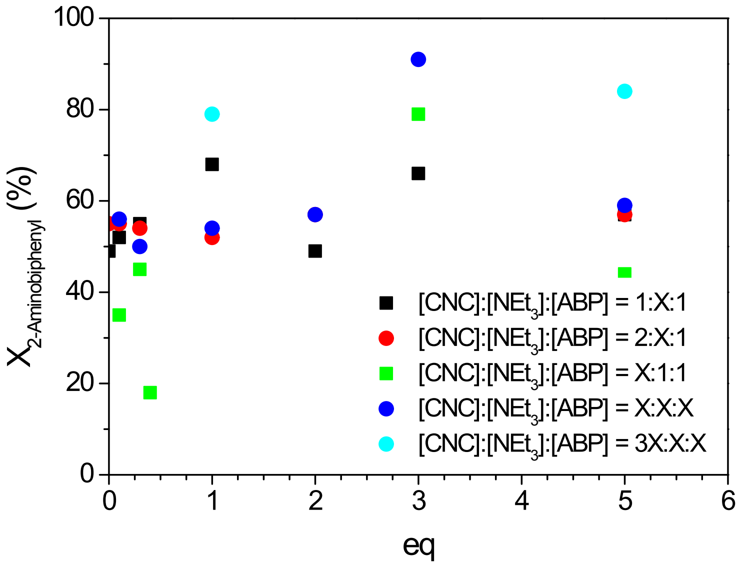

Figure S 12. Influence of reaction composition with NEt_3 as the base (X=eq).

The solvent has the strongest impact on the results. From the yields obtained for different solvents, e.g. heptane, EtOH, DCM, or THF, it is obvious that aprotic solvents should be favoured for the condensation reaction. Protic solvents like ethanol or water can support the hydrolysis of CNC.

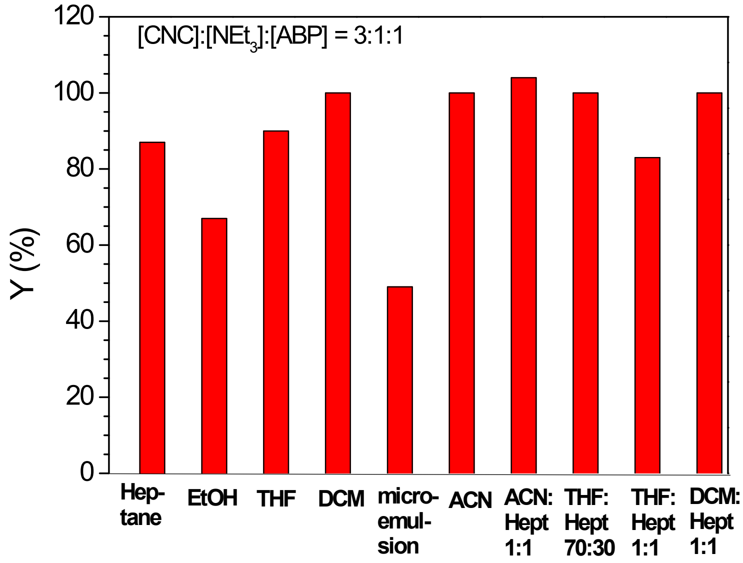

Figure S 13. Influence of the solvent on the yield for the condensation of ABP at constant $[CNC]:[NEt_3]:[ABP]$ ratio of 3:1:1.